J. Fluid Mech. (2006), vol. 567, pp. 361–378.
doi:10.1017/S0022112006002370 Printed in the United Kingdom

Steady axisymmetric creeping plumes above a planar boundary. Part 1. A point source

By ROBERT J. WHITTAKER AND JOHN R. LISTER

Institute of Theoretical Geophysics, Department of Applied Mathematics and Theoretical Physics, University of Cambridge, Wilberforce Road, Cambridge, CB3 0WA, UK

(Received 1 September 2005 and in revised form 10 May 2006)

Asymptotic solutions are obtained for the rise of an axisymmetric hot plume from a localized source at the base of a half-space filled with very viscous fluid. We consider an effectively point source, generating a prescribed buoyancy flux B, and show that the length scale of the plume base is $z_0 = (32\pi\kappa^2\nu/B)$, where ν and κ are the kinematic viscosity and thermal diffusivity. The internal structure of the plume for $z \gg z_0$ is found using stretched coordinates, and this is matched to a slender-body expansion for the external Stokes flow. Solutions are presented for both rigid (no-slip) and free-slip (no tangential stress) conditions on the lower boundary. In both cases we find that the typical vertical velocity in the plume increases slowly with height as $(B/\nu)^{1/2}[\ln(z/z_0)]^{1/2}$, and the plume radius increases as $(zz_0)^{1/2}[\ln(z/z_0)]^{-1/4}$.

1. Introduction

Steady plumes above a heated source are an important and canonical topic in convection. The existence of localized plume structures in the Earth's mantle (first suggested by Morgan 1971) provides one motivation to study the case of infinite Prandtl number. However, our results may have wider applications to other situations involving very viscous fluids, for example in magma chambers and industrial processes such as glass manufacture (Krause & Loch 2002).

There have been various investigations of viscous plumes with both constant and temperature-dependent viscosity. These have involved experiments, numerical simulations, and analytical models. For example, recent experimental work on viscous plumes has included that of Kaminski & Jaupart (2003), who focused mainly on the evolution of starting plumes, and Kerr & Mériaux (2004), who considered the effects of an externally applied shear flow on the trajectory of a rising plume.

On the theoretical side, four previous studies of isoviscous plumes are of particular relevance to the work presented here and in Part 2 of this study (Whittaker & Lister 2006). A detailed analysis of an infinite-Prandtl-number plume at large Rayleigh number in two-dimensional convection was carried out by Roberts (1977). In particular, by coupling the motion of the plume to the thermal boundary layer directly above a distributed source, Roberts found asymptotic relationships between the Nusselt and Rayleigh numbers for a heated strip.

An isolated axisymmetric plume in an unbounded volume of large-Prandtl-number fluid was studied by Worster (1986). There is no pure Stokes flow solution for an isolated plume in an unbounded domain, for much the same reason that Oseen corrections are required for the problem of an infinite translating cylinder (see Lamb 1911). Inertia is important in the far field, and is required to provide a normalization

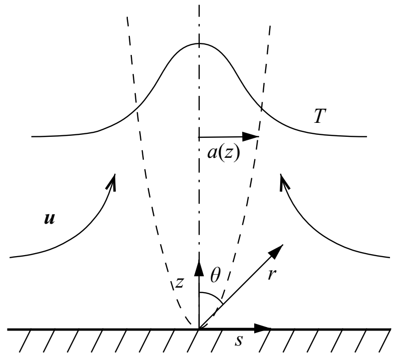

FIGURE 1. A definition sketch for the point-source plume under investigation, showing the coordinates s, z, r and θ that will be used to describe it, the plume radius $a(z)$, temperature profile $T(s, z)$, and the velocity in the fluid $\boldsymbol{u}$.

for the interior flow. Worster (1986) derived a matched asymptotic expansion for $Pr \gg 1$, comprising a viscous–buoyancy dominated plume, and an inertia–viscous dominated outer flow.

Olson, Schubert & Anderson (1993) provide an idealized model for one of the problems we consider in Part 2: the distributed source with a free-slip boundary condition. Finally, the related problem of an axisymmetric convection cell with free-slip walls has been considered by Umemura & Busse (1989). The cell was forced by a fixed temperature difference between the horizontal boundaries, and matched asymptotic solutions were derived for the interior flow, a central plume, and the various boundary layers adjacent to the walls.

Various authors, including Olson *et al.* (1993) and Loper & Stacey (1983), have also considered the structure of plumes with variable viscosity, with emphasis on their application to mantle convection. Such studies have tended to concentrate on the case of a very large viscosity contrast between the plume core and outer fluid. This leads to the vertical motion being confined to a narrow conduit, surrounded by a much wider thermal halo.

In this paper, we consider a steady isoviscous axisymmetric plume rising above a plane boundary from a point source of specified buoyancy flux (see figure 1). The problem is solved by considering separately a slender plume region (in which boundary-layer approximations can be employed), and an outer Stokes flow (in which the temperature is uniform). In Part 2, we consider the effects of a finite source at large Rayleigh number, and examine the thermal boundary layer that forms above it. The assumption of constant viscosity is obviously a restriction, but it allows considerable progress to be made in understanding the plume structure. Some discussion of the effects of temperature-dependent viscosity can be found in § 6.

Much of the work presented here and in Part 2 is essentially the axisymmetric version of the two-dimensional planar problem studied by Roberts (1977). However, the change in geometry has a significant effect on the nature of the solution. This is mainly attributable to the solutions for the outer flow having differing behaviours near the axis: with a planar geometry, the inner limit of the outer vertical velocity is essentially independent of the width of the plume; with an axisymmetric geometry, we have a logarithmic singularity (see § 4) so the plume width is now coupled directly with the vertical velocity inside the plume. This coupling complicates the solution somewhat.

The point-source problem addressed here is also similar to that studied by Worster (1986) in an infinite fluid. However, the presence of a lower boundary in our problem means that the introduction of inertial terms in the far field is no longer necessary to balance the vertical force. This can be understood by considering the flow with a planar boundary as the sum of that due to the plume's buoyancy forces in the absence of the boundary, and that due to an image system below the plane (see § 4.1). The image system cancels the leading-order Stokeslet terms and causes the far-field velocity to decay more rapidly. Hence, while Worster's equations for the inner region are very similar to those which arise here, there are major differences in the outer flow, to which the inner solution is matched.

This paper is organized as follows. A detailed description of the problem and some initial scaling arguments for the main features of the flow are presented in § 2. In § § 3–5, we solve the problem by matching an inner plume region to an outer isothermal Stokes flow in an asymptotic solution for a slender plume. Since the slender-body expansion is only in inverse powers of a logarithm and hence slowly converging, we take the trouble to calculate the first-order corrections to the leading-order terms. Finally, some discussion and concluding remarks are presented in § 6. Some of the techniques developed in this paper are used further in Part 2, in which we consider the related problem of the flow and temperature fields due to a distributed source.

2. Formulation and scaling

2.1. *Governing equations and boundary conditions*

We consider a steady vertical plume in the half-space $z > 0$ above a horizontal boundary $z = 0$. The plume is generated by a localized source of heat close to the boundary, and the far field is assumed to be quiescent with a background temperature T_0. Inertial effects are considered to be negligible, and the Boussinesq approximation employed. We also assume that the kinematic viscosity ν is constant, and that the plume remains axisymmetric. A sketch of the situation under consideration, along with the coordinate systems used, is shown in figure 1.

The governing equations are the Stokes equations for incompressible flow, and the steady advection–diffusion equation for heat. We use $b = g\beta(T - T_0)$ to describe the buoyancy distribution, where β is the coefficient of linear thermal expansion and g is the acceleration due to gravity. The governing equations are thus

$$\nu\nabla^2\boldsymbol{u} = \nabla p - b\hat{\boldsymbol{e}}_z, \tag{2.1}$$

$$\nabla\cdot\boldsymbol{u} = 0, \tag{2.2}$$

$$(\boldsymbol{u}\cdot\nabla)\, b = \kappa\nabla^2 b, \tag{2.3}$$

where $\hat{\boldsymbol{e}}_z$ is the unit vertical vector, κ is the thermal diffusivity, and p is a modified pressure.

To satisfy the far-field conditions, we require $\boldsymbol{u} \to \boldsymbol{0}$ and $b \to 0$ as $r \to \infty$ with θ fixed and $0 < \theta \leqslant \pi/2$. We shall consider the effect of both rigid ($\boldsymbol{u} = \boldsymbol{0}$) and free-slip ($\hat{\boldsymbol{e}}_z \cdot \boldsymbol{u} = 0$, $\hat{\boldsymbol{e}}_z \cdot \nabla\boldsymbol{u} \times \hat{\boldsymbol{e}}_z = \boldsymbol{0}$) boundary conditions on the horizontal boundary $z = 0$.

Conservation of heat allows us to define a vertical buoyancy flux B, which is independent of the height z. Assuming that vertical advection dominates vertical diffusion, we have

$$B = 2\pi \int_0^\infty wb\, s\, \mathrm{d}s, \tag{2.4}$$

where $w = \boldsymbol{u}\cdot\hat{\boldsymbol{e}}_z$ is the vertical velocity, and s is the horizontal radial coordinate. The invariance of B may be derived from (2.2) and (2.3) by using the boundary conditions and neglecting κb_{zz}.

Here we consider a point source with a prescribed heat flux, and so B is simply a fixed parameter of the system. For the distributed source considered in Part 2, B must be determined by solving a thermal boundary-layer problem in the neighbourhood of the source.

2.2. *Separation of scales*

Sufficiently far from the source, we expect a slender thermal plume of typical radius $a(z)$, surrounded by an outer region in which $b \approx 0$. Within the inner plume region, cylindrical polar coordinates (s, ϕ, z) are used, and a scaled radial coordinate $\xi = s/a(z)$ is introduced. For sufficiently large z, it is expected that $a(z) \ll z$ and boundary-layer approximations can be employed.

Since the temperature is effectively uniform in the outer region, the velocity there will be a Stokes flow with zero body force. It is driven only by the effect of the buoyancy force in the plume, which is transmitted through the matching of the two regions. We therefore expect the outer flow to have an $O(1)$ aspect ratio, and the use of spherical polar coordinates (r, θ, ϕ) is found to be convenient.

Solutions for the inner and outer regions are derived in § 3 and § 4, respectively. The traction and velocity must be matched between the two regions in an intermediate zone characterized by $\theta \ll 1$ and $\xi \gg 1$. This is described in § 5.

2.3. *Scaling estimates*

Simple scaling estimates can be employed to describe the plume. From the advection–diffusion equation (2.3) and conservation of buoyancy (2.4) we obtain within the plume

$$\frac{w}{z} \sim \frac{\kappa}{a^2}, \quad wba^2 \sim B, \quad \text{whence} \quad b \sim \frac{B}{\kappa z}. \tag{2.5a–c}$$

Slender-body theory (see, for example, Cox 1970; Leal 1992, pp. 247–251) can be used to provide an estimate for the rise velocity. This is a local calculation based on a line of Stokeslets with local density $F \sim ba^2$. The leading-order result that

$$w \sim \frac{F}{2\pi\nu} \ln\left(\frac{z}{a}\right) \tag{2.6}$$

is unaffected by the precise form of the tangential velocity condition imposed on the lower boundary. While the tangential component of the boundary condition does not affect (2.6), the normal component $\boldsymbol{u}\cdot\hat{\boldsymbol{e}}_z = 0$, which reflects the inhibition of vertical flow due to the presence of the boundary, is vital. Without something to balance the vertical force, inertial effects in the far field would dominate, and there would be no Stokes-flow solution. We would then be back to the situation analysed by Worster (1986).

Combining (2.5) and (2.6), and introducing a length scale $z_0 \propto (\nu\kappa^2/B)^{1/2}$, we obtain

$$w \sim \left(\frac{B}{\nu}\right)^{1/2} \left[\ln\left(\frac{z}{a}\right)\right]^{1/2}, \quad F \sim \frac{(B\nu)^{1/2}}{[\ln(z/a)]^{1/2}}, \quad a \sim \frac{(z_0\, z)^{1/2}}{[\ln(z/a)]^{1/4}}. \tag{2.7a–c}$$

Finally, we argue that the vertical velocity inside the plume is dominated by a plug flow $w_0(z)$, with the radial variation $\tilde{w}(s, z)$ across the plume having a much smaller magnitude. By substituting the scalings for a and b into the Stokes equation (2.1), we obtain

$$\frac{\nu \tilde{w}}{a^2} \sim b \Rightarrow \tilde{w} \sim \left(\frac{B}{\nu}\right)^{1/2} [\ln(z/z_0)]^{-1/2} . \tag{2.8}$$

Therefore $\tilde{w}$ will indeed be much smaller than w_0 for $z \gg z_0$. The separation of magnitudes, $a \ll z$ and $\tilde{w} \ll w_0$, will now be exploited to derive inner and outer expansions for the plume and the surrounding fluid.

3. The inner solution

3.1. *Series expansion*

Introducing a Stokes streamfunction, $\psi(s, z)$, we write the horizontal and vertical velocities inside the plume as

$$u = \boldsymbol{u} \cdot \hat{\boldsymbol{e}}_s = -\frac{1}{s}\frac{\partial \psi}{\partial z}, \quad w = \boldsymbol{u} \cdot \hat{\boldsymbol{e}}_z = \frac{1}{s}\frac{\partial \psi}{\partial s}, \tag{3.1}$$

From the advection–diffusion balance expressed in (2.5*a*), we expect the plume radius to scale as $a = (4\kappa z/w_0)^{1/2}$, where $w_0(z)$ is the (as yet unknown) leading-order vertical velocity, which is horizontally uniform by (2.8). We therefore introduce a scaled radial variable ξ, defined by

$$\xi = \frac{s}{a} = s\left(\frac{w_0(z)}{4\kappa z}\right)^{1/2} . \tag{3.2}$$

Based on the scalings of §2.3, we write the streamfunction and buoyancy fields in terms of ξ and z. It is found to be convenient to keep the factor of 4 with κ, and to introduce a factor of 2π in the expression for b. We therefore define

$$\psi = 4\kappa z\, f(\xi\, ; z), \qquad b = \frac{B}{2\pi}\frac{g(\xi\, ; z)}{4\kappa z} . \tag{3.3a, b}$$

With the definitions (3.2) and (3.3*a*), the vertical velocity is given by

$$w = \frac{w_0}{\xi}\frac{\partial f}{\partial \xi} , \tag{3.4}$$

so we require $f'(\xi\, ; z) \sim \xi$ at leading order, where a prime ($'$) denotes differentiation with respect to ξ. More precisely, we want this to hold as $z \to \infty$ with ξ fixed, corresponding to an asymptotically uniform vertical flow in each cross-section of the plume.

The expressions (3.3) for ψ and b are now substituted into the governing equations (2.1) and (2.3), and the buoyancy normalization (2.4). After applying standard boundary-layer approximations to neglect the vertical derivatives in the Laplacians and the vertical gradient of the modified pressure, we obtain

$$\frac{1}{\xi}\frac{\partial}{\partial \xi}\left(\xi \frac{\partial}{\partial \xi}\left(\frac{1}{\xi}\frac{\partial f}{\partial \xi}\right)\right) = -\epsilon g, \tag{3.5}$$

$$f'(-g + z g_z) - (f + z f_z)\, g' = \tfrac{1}{4}(\xi g')', \tag{3.6}$$

$$\int_0^\infty g\, f'\, \mathrm{d}\xi = 1, \tag{3.7}$$

where we have also introduced

$$\epsilon(z) = \frac{B}{2\pi\nu w_0^2}. \tag{3.8}$$

For $\epsilon \ll 1$ it is natural to consider the expansions

$$f(\xi\,;z) = f_0(\xi) + \epsilon(z) f_1(\xi) + O(z\epsilon_z, \epsilon^2), \tag{3.9}$$

$$g(\xi\,;z) = g_0(\xi) + \epsilon(z) g_1(\xi) + O(z\epsilon_z, \epsilon^2). \tag{3.10}$$

From the previous scalings (2.7), we expect to find that $\epsilon(z) \sim (\ln z)^{-1}$. For the time being, we need only assume that $z\epsilon_z \ll \epsilon$ to obtain the correct ordering of terms in the heat equation (3.6). Since ϵ is expected to be only logarithmically small in z, we shall calculate both the leading-order and the $O(\epsilon)$ terms.

We note that there are also other eigenmodes of the heat equation (3.6), which are the product of a negative integer power of z and a function of ξ. These modes are investigated in Appendix A, where it is argued that they decay algebraically rapidly with z, and thus become insignificant compared with the terms shown in (3.10).

3.2. *The leading-order equations*

We now substitute the expansions (3.9) and (3.10) into (3.5)–(3.7). Equating the leading-order terms in ϵ, we obtain

$$\frac{1}{\xi}\frac{\partial}{\partial \xi}\left(\xi \frac{\partial}{\partial \xi}\left(\frac{1}{\xi}\frac{\partial f_0}{\partial \xi}\right)\right) = 0, \tag{3.11}$$

$$(\xi g_0')' + 4(f_0' g_0 + f_0 g_0') = 0, \tag{3.12}$$

$$\int_0^\infty g_0 f_0' \,\mathrm{d}\xi = 1. \tag{3.13}$$

The leading-order Stokes equation (3.11) is readily solved to give

$$f_0(\xi) = \tfrac{1}{2}\xi^2. \tag{3.14}$$

Two constants of integration are used to satisfy regularity conditions at $\xi = 0$ (corresponding to no mass source and no forcing singularity), and the third is set by the requirement that the vertical velocity (3.4) is precisely $w_0(z)$ at leading order.

We now substitute $f_0(\xi)$ into (3.12) and (3.13). The leading-order heat equation (3.12) is integrated to obtain

$$g_0(\xi) = 2\exp(-\xi^2). \tag{3.15}$$

One constant of integration is set to avoid a singularity at $\xi = 0$, and the other so that the normalization condition (3.13) is satisfied.

Equations (3.14) and (3.15) constitute the leading-order solution for the velocity and temperature fields inside the plume.

3.3. *The first-order equations*

Equating the $O(\epsilon)$ terms in (3.5)–(3.7), we obtain

$$\frac{1}{\xi}\frac{\partial}{\partial \xi}\left(\xi \frac{\partial}{\partial \xi}\left(\frac{1}{\xi}\frac{\partial f_1}{\partial \xi}\right)\right) = -g_0, \tag{3.16}$$

$$(\xi g_1')' + 4(f_0' g_1 + f_0 g_1') = -4(f_1' g_0 + f_1 g_0'), \tag{3.17}$$

$$\int_0^\infty (g_0 f_1' + g_1 f_0') \,\mathrm{d}\xi = 1. \tag{3.18}$$

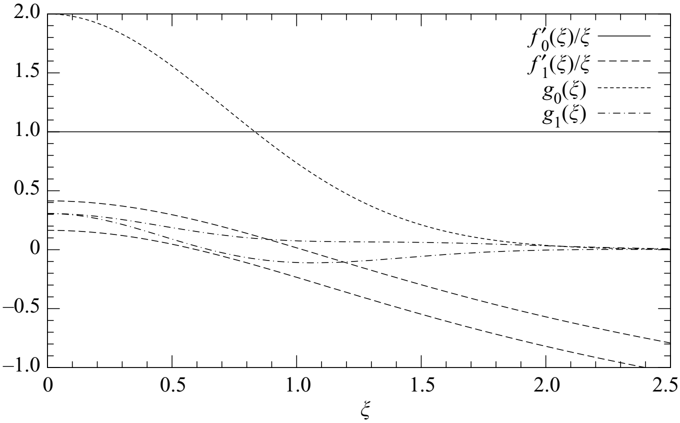

FIGURE 2. The leading and first-order profiles of the dimensionless temperature g and vertical velocity f'/ξ within the plume. The two versions of the first-order functions f_1 and g_1 are for the values (5.10) of the constant A that arise with free-slip and rigid boundary conditions. The rigid case corresponds to the lower velocity and higher temperature. Note the logarithmic behaviour in the velocity f'/ξ as $\xi \to \infty$.

These are solved in an analogous manner to the leading-order equations (3.11)–(3.13). Equation (3.16) is integrated to give

$$f_1(\xi) = \tfrac{1}{2}A\xi^2 - \tfrac{1}{4}\xi^2(2\ln\xi + \mathrm{Ei}(\xi^2) + \gamma - 1) + \tfrac{1}{4}(\exp(-\xi^2) - 1), \tag{3.19}$$

where $\mathrm{Ei}(x) = \int_1^\infty t^{-1}\mathrm{e}^{-xt}\,\mathrm{d}t$, and $\gamma = 0.5772\ldots$ is Euler's constant. As before, two constants of integration are set by regularity conditions at $\xi = 0$. The third constant A sets the magnitude of a vertical plug flow proportional to $\epsilon(z)$, and can be found only by matching with the outer solution. As we shall see, the value of A depends on the boundary condition on the tangential velocity (free-slip or rigid) at $z = 0$.

Equation (3.17) can now be integrated subject to the normalization condition (3.18) to obtain a somewhat complicated closed-form expression for $g_1(\xi)$. A graph of g_1 together with the other inner functions is presented in figure 2. Higher-order terms may also be calculated, but will not be reported here.

Having calculated f_0 and f_1, we substitute the series (3.9) into (3.4) to obtain

$$w \sim w_0(z)\left[1 + \epsilon(z)\left(-\ln\xi - \tfrac{1}{2}\mathrm{Ei}(\xi^2) + A - \frac{\gamma}{2}\right) + \cdots\right]. \tag{3.20}$$

For matching with the outer solution, we require the asymptotic form of this expression as $\xi \to \infty$. In this respect, observe that $\mathrm{Ei}(\xi^2)$ decays exponentially as $\xi^{-2}\exp(-\xi^2)$.

4. The outer solution

4.1. *Integral representation*

The outer velocity field is completely determined by the buoyancy distribution $b(\boldsymbol{x})$ of the inner solution, together with the conditions imposed on the horizontal boundary. The flow field can be expressed in terms of this forcing using an extension to the standard Stokeslet integral representation.

A general solution for Stokes flows in the presence of a rigid plane boundary was first given by Lorentz (1907). For a single Stokeslet, Blake (1971) showed that the flow may be expressed as the sum of a finite number of singularities as shown in

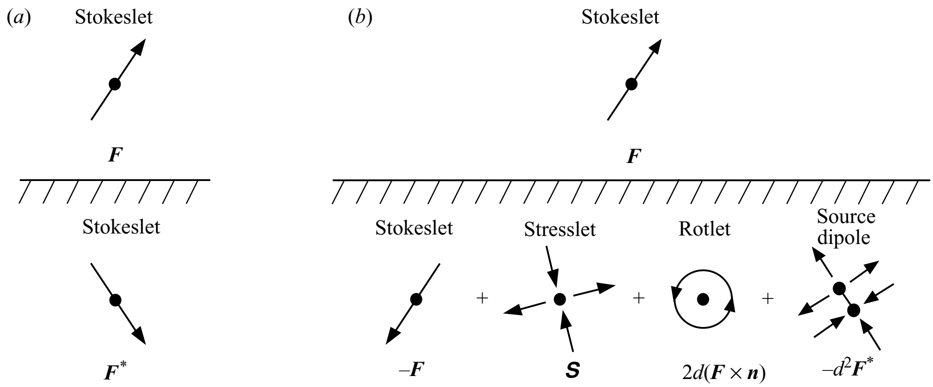

FIGURE 3. The image system for a Stokeslet located a distance d above a plane boundary $\boldsymbol{x}\cdot\boldsymbol{n}=0$. The systems for both ($a$) free-slip and ($b$) rigid boundary conditions are shown. The mirrored force is given by $\boldsymbol{F}^*=\boldsymbol{F}\cdot(\boldsymbol{I}-2\boldsymbol{nn})$, and the stresslet moment is $\boldsymbol{S}=-d(\boldsymbol{F}^*\boldsymbol{n}+\boldsymbol{nF}^*-\frac{2}{3}(\boldsymbol{n}\cdot\boldsymbol{F}^*)\boldsymbol{I})$.

figure 3 (see also Pozrikidis 1992, §3.3). Solutions for a buoyancy distribution can then be constructed by linear superposition as

$$\boldsymbol{u}(\boldsymbol{x})=\frac{1}{8\pi\nu}\int_{z'>0} b(\boldsymbol{x}')\,\hat{\boldsymbol{e}}_z\cdot\boldsymbol{K}(\boldsymbol{x};\boldsymbol{x}')\,\mathrm{d}^3x', \tag{4.1}$$

where $\boldsymbol{K}(\boldsymbol{x};\boldsymbol{x}')=\boldsymbol{J}(\boldsymbol{x}-\boldsymbol{x}')+\boldsymbol{J}^*(\boldsymbol{x}-\boldsymbol{R}\cdot\boldsymbol{x}')$. Here, $\boldsymbol{J}$ is the Oseen tensor, given by

$$\boldsymbol{J}(\boldsymbol{x})=\left(\frac{\boldsymbol{I}}{|\boldsymbol{x}|}+\frac{\boldsymbol{xx}}{|\boldsymbol{x}|^3}\right), \tag{4.2}$$

$\boldsymbol{J}^*$ is the Green's function for the corresponding image system at the mirror point $\boldsymbol{R}\cdot\boldsymbol{x}'$, and $\boldsymbol{R}=\boldsymbol{I}-2\hat{\boldsymbol{e}}_z\hat{\boldsymbol{e}}_z$ is the reflection tensor about $z=0$.

For the case that the forcing is everywhere perpendicular to the plane, the image Green's function $\boldsymbol{J}^*$ simplifies somewhat. For the free-slip boundary condition, we find that $\hat{\boldsymbol{e}}_z\cdot\boldsymbol{J}^*(\boldsymbol{x})=-\hat{\boldsymbol{e}}_z\cdot\boldsymbol{J}(\boldsymbol{x})$. For the rigid boundary condition,

$$\hat{\boldsymbol{e}}_z\cdot\boldsymbol{J}^*(\boldsymbol{x})=-\hat{\boldsymbol{e}}_z\cdot\boldsymbol{J}(\boldsymbol{x})-\frac{3(\boldsymbol{x}\cdot\boldsymbol{S}\cdot\boldsymbol{x})\boldsymbol{x}}{|\boldsymbol{x}|^5}+2z'^2\hat{\boldsymbol{e}}_z\cdot\left(-\frac{\boldsymbol{I}}{|\boldsymbol{x}|^3}+\frac{3\boldsymbol{xx}}{|\boldsymbol{x}|^5}\right), \tag{4.3}$$

where $\boldsymbol{S}=2z'(3\hat{\boldsymbol{e}}_z\hat{\boldsymbol{e}}_z-\boldsymbol{I})/3$ is the stresslet moment and the final term represents a source dipole. (The absence of a rotlet term in this case may be deduced by symmetry considerations alone.)

4.2. *Multi-pole expansion*

Equation (4.1) holds for a general buoyancy distribution, but we now exploit the fact that the buoyancy in the plume is confined to a narrow region of radius $O(a)$, where $a\ll z$. We can then consider a multi-pole expansion, valid for locations outside the plume. Since the buoyancy distribution is confined in the radial direction but not the vertical, we expand in terms of the radial moments, leaving the vertical integrals intact. We obtain

$$\boldsymbol{u}(\boldsymbol{x})=\frac{1}{8\pi\nu}\int_0^\infty F(z')\,\hat{\boldsymbol{e}}_z\cdot\boldsymbol{K}(\boldsymbol{x};z'\hat{\boldsymbol{e}}_z)\,\mathrm{d}z' +\frac{1}{8\pi\nu}\int_0^\infty M(z')\,\hat{\boldsymbol{e}}_z\cdot\nabla_{\mathrm{h}}^2\boldsymbol{K}(\boldsymbol{x};z'\hat{\boldsymbol{e}}_z)\,\mathrm{d}z'+\cdots, \tag{4.4}$$

where

$$F(z) = 2\pi \int_0^\infty b(s,z)\, s\, \mathrm{d}s = \frac{B}{w_0} \int_0^\infty g(\xi\,; z)\, \xi\, \mathrm{d}\xi, \tag{4.5}$$

$$M(z) = \frac{\pi}{2} \int_0^\infty b(s,z)\, s^3\, \mathrm{d}s = \frac{B}{w_0} \frac{a^2}{4} \int_0^\infty g(\xi\,; z)\, \xi^3\, \mathrm{d}\xi. \tag{4.6}$$

These moments of the buoyancy distribution may be expanded as series in ϵ. For the vertical force density F (which turns out to be of greatest interest), we can use the normalization integrals (3.13) and (3.18) to evaluate each term F_k without requiring full knowledge of the corresponding function $g_k(\xi)$. Thus,

$$\begin{aligned} F(z) &= \frac{B}{w_0}\left(\int_0^\infty g_0(\xi)\, \xi\, \mathrm{d}\xi + \epsilon(z) \int_0^\infty g_1(\xi)\, \xi\, \mathrm{d}\xi + \cdots\right) \\ &= \frac{B}{w_0}\left(1 - \epsilon(z) \int_0^\infty g_0(\xi) f_1'(\xi)\, \mathrm{d}\xi + \cdots\right) \\ &= \frac{B}{w_0}\left(1 - \epsilon(z)\left(A - \tfrac{1}{2}\ln 2\right) + \cdots\right). \end{aligned} \tag{4.7}$$

This manipulation is possible because the leading-order velocity is horizontally uniform within the plume, and so pairs of terms in the buoyancy flux and force integrals involve the same moments of $g_k(\xi)$. We can therefore swap the integral of $\xi g_k(\xi)$ for one involving only terms of the form $f_i'(\xi) g_j(\xi)$ with $i \leqslant k$ and $j < k$. In particular, the leading-order component $F_0(z) = B/w_0(z)$ is independent of the radial structure $g(\xi\,; z)$ of the buoyancy distribution. At the next order, it is not necessary to have found g_1 explicitly in order to calculate F_1.

4.3. *Evaluation of the outer velocity field*

The detailed calculation of the outer velocity field is best left until the form of $w_0(z)$ has been determined, and is presented in Appendix B. For now, we concentrate on the asymptotic form of the outer solution as $r/z \to 0$, since this is all that is required for matching with the inner solution.

Defining $K(s, z; z') = \hat{\boldsymbol{e}}_z \cdot \boldsymbol{K}(\boldsymbol{x}, z'\hat{\boldsymbol{e}}_z) \cdot \hat{\boldsymbol{e}}_z$, the vertical component of (4.4) is given by

$$8\pi\nu\, w(s,z) = \int_0^\infty F(z')\, K(s, z; z')\, \mathrm{d}z' + \int_0^\infty M(z')\, \nabla_{\mathrm{h}}^2 K(s, z; z')\, \mathrm{d}z' + \cdots. \tag{4.8}$$

With the free-slip boundary condition

$$K(s, z; z') = \frac{s^2 + 2(z - z')^2}{(s^2 + (z - z')^2)^{3/2}} - \frac{s^2 + 2(z + z')^2}{(s^2 + (z + z')^2)^{3/2}}, \tag{4.9}$$

whereas for the rigid case

$$K(s, z; z') = \frac{s^2 + 2(z - z')^2}{(s^2 + (z - z')^2)^{3/2}} - \frac{s^2 + 2(z + z')^2}{(s^2 + (z + z')^2)^{3/2}} + \frac{2zz'(s^2 - 2(z + z')^2)}{(s^2 + (z + z')^2)^{5/2}}. \tag{4.10}$$

The first term on the right-hand sides of (4.9) and (4.10) represents a line of Stokeslets along the plume axis. It is of the same asymptotic form as the integrand in slender-body theory, and gives a logarithmically large contribution to the velocity. The second term in each equation represents the image Stokeslet. It cancels the $O(z'^{-1})$ behaviour of the Stokeslets, which would otherwise prevent the integrals from converging as $z' \to \infty$. For the rigid case, there is also a third term which represents the higher-order singularities (stresslet and source dipole) in the image system.

We are interested primarily in the region $s \ll z$. Then for $|z' - z| \ll z$, $K(s, z; z')$ is dominated by the first term, and so behaves like the usual integrand in slender-body theory. However, away from this region the decay is faster: as $z' \to \infty$, we have $K = O(z'^{-2})$ for the free-slip case and $K = O(z'^{-3})$ for the rigid case; as $z' \to 0$, we have $K = O(z')$ for the free-slip case and $K = O(z'^2)$ for the rigid case.

From the estimate (2.7a) for w_0, we expect F and M to be slowly varying logarithmic functions of z'. As will be checked later, we therefore make only an asymptotically small error by approximating $F(z')$ and $M(z')$ by their values at $z' = z$, where the dominant contribution to the integrals occurs.

The factors $F(z)$ and $M(z)$ can then be moved outside the integrals, leaving integrals of K and its horizontal derivatives. These may be evaluated explicitly, and the behaviour as $s/z \to 0$ determined. We find that

$$\int_0^\infty K(s, z; z')\,\mathrm{d}z' = -4\ln\left(\frac{s}{z}\right) + 4(\ln 2 - \delta) + O\left(\frac{s^2}{z^2}\right), \tag{4.11}$$

$$\int_0^\infty \nabla_\mathrm{h}^2 K(s, z; z')\,\mathrm{d}z' = \frac{4}{z^2}\left[(1 + 2\delta) + O\left(\frac{s^2}{z^2}\right)\right], \tag{4.12}$$

where $\delta = 1/2$ for the free-slip case, and $\delta = 1$ for the rigid case. The integrals of higher derivatives of K (corresponding to higher-order moments of the inner buoyancy distribution) are at most $O(z^{-4})$.

Combining (4.7), (4.8) and (4.11), we find that

$$w \sim \frac{B}{2\pi\nu w_0(z)}\left[1 - \epsilon(z)\left(A - \tfrac{1}{2}\ln 2\right) + \cdots\right]\left[-\ln\left(\frac{s}{z}\right) + (\ln 2 - \delta) + \cdots\right], \tag{4.13}$$

at the inner edge of the outer solution. To obtain this expression, we have approximated $F(z')$ by $F(z)$ as mentioned above, and also neglected any contributions from terms involving $M(z)$. The errors generated by these and the other approximations are quantified later.

5. Matching the vertical velocity

The temperature, velocity, and traction from the inner and outer solutions must now be matched in the intermediate region given by $\xi \ll 1$ and $\theta \ll 1$. However, the temperature is already taken care of (to the orders in which we are interested) since it is exponentially small at the outer edge of the inner solution, and is assumed to be zero throughout the outer solution. The traction is also taken care of, since it is directly related to the internal buoyancy of the plume, which was used to derive the outer solution.

This leaves only the velocity to be matched. We need only match the vertical component, since the horizontal component will follow by incompressibility. Formally, we should use an intermediate variable for the matching but, for simplicity, we shall just re-write the outer solution in terms of the inner variables (ξ, z). It will suffice to keep track of the range of ξ in the matching region, and to ensure that the neglected terms are strictly smaller than those retained.

5.1. *Inner and outer expansions*

First, we observe that

$$\frac{s}{z} = \xi\left(\frac{4\kappa}{z w_0}\right)^{1/2} = \xi\epsilon^{1/4}\left(\frac{z}{z_0}\right)^{-1/2}, \quad \text{where } z_0 = \left(\frac{32\pi\kappa^2\nu}{B}\right)^{1/2}. \tag{5.1}$$

A quick matching of the leading-order behaviour of the vertical velocity between the inner (3.20) and outer (4.13) solutions gives

$$w_0(z) \sim -\frac{B}{2\pi\nu w_0} \ln\left(\frac{s}{z}\right) = w_0\epsilon \ln\left(\xi^{-1}\epsilon^{-1/4}\left(\frac{z}{z_0}\right)^{1/2}\right), \tag{5.2}$$

where we have made use of (3.8) which defines ϵ in terms of w_0. We thus obtain $\epsilon(z) \sim 2\,[\ln(z/z_0)]^{-1}$ and $w_0(z) \sim (B/4\pi\nu)^{1/2}\,[\ln(z/z_0)]^{1/2}$, which is consistent with the scaling estimates of § 2.3.

Now the form of ϵ is known, we are in a position to match the velocities formally, ordering the various terms correctly. Note that the matching region corresponds to $a \ll s \ll z$, or equivalently $1 \ll \xi \ll \epsilon^{-1/4}(z/z_0)^{1/2}$.

From (3.20), we obtain

$$\frac{w}{w_0} \sim 1 - \epsilon \ln \xi + \epsilon\left(A - \frac{\gamma}{2}\right) + \cdots, \tag{5.3}$$

at the outer edge of the inner plume solution. The correction terms are $O(\epsilon^2)$ from neglecting terms f_2 and above, $O(\epsilon\,\xi^{-2}\mathrm{e}^{-\xi^2})$ from the large-ξ approximation, and $O(\xi^2\epsilon^{1/2}z_0/z)$ from the use of a boundary-layer approximation within the plume.

From the inner limit of the outer solution (4.13), we obtain

$$\frac{w}{w_0} \sim \tfrac{1}{2}\epsilon \ln\left(\epsilon^{-1/2}\frac{z}{z_0}\right) - \epsilon \ln \xi + \epsilon(\ln 2 - \delta) - \tfrac{1}{2}\epsilon^2\left(A - \tfrac{1}{2}\ln 2\right)\ln\left(\epsilon^{-1/2}\frac{z}{z_0}\right) + \cdots. \tag{5.4}$$

The correction terms are $O(\epsilon^2)$ from the remaining contribution to F_1, $O(\epsilon^3\ln(z/z_0))$ from higher-order terms in the expansion of F, $O(\xi^2\epsilon^{1/2}z_0/z)$ from the truncation of the expansion of the K integral, $O(\epsilon^{1/2}z_0/z)$ from neglecting the contribution from M and higher moments, and $O(\epsilon/\ln(z/z_0))$ from approximating $F(z')$ by $F(z)$.

By a slight narrowing of the matching region to $\epsilon^{1/2} \lesssim \xi \lesssim \epsilon^{3/4}(z/z_0)^{1/2}$, we can ensure that the errors in the inner and outer expansions are all $O(\epsilon^2)$ or smaller. This allows us to match (5.3) and (5.4) up to $O(\epsilon)$.

5.2. *Formal matching*

Comparing the leading-order terms in (5.3) and (5.4), we obtain

$$1 = \tfrac{1}{2}\epsilon \ln\left(\epsilon^{-1/2}\frac{z}{z_0}\right) + O(\epsilon). \tag{5.5}$$

Note that we have some freedom in choosing ϵ to satisfy this equation, since any $O(\epsilon)$ discrepancy is permitted. We make the most simple and convenient choice by defining $\epsilon(z)$ to be the smaller of the two roots of

$$\frac{2}{\epsilon} + \tfrac{1}{2}\ln\epsilon = \ln\left(\frac{z}{z_0}\right), \tag{5.6}$$

(assuming that $z/z_0 \geqslant 2\sqrt{\mathrm{e}}$). Different choices would only change ϵ slightly (the difference not appearing until the third term in the expansion (5.7)). They would also result in an extra term appearing in the $O(\epsilon)$ matching below, which in turn would alter the value of A given in (5.10). However, when the full solution is reconstructed these two effects necessarily cancel each other out.

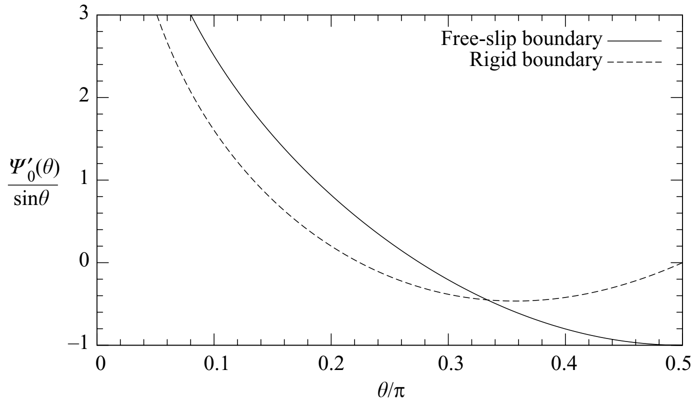

FIGURE 4. The dimensionless leading-order radial velocity as a function of polar angle (see Appendix B). The dimensional form is given by $u_r(r,\theta) \sim B^{1/2}[4\pi\nu \ln(r/z_0)]^{-1/2}\, \Psi_0'(\theta)/\sin\theta$. Note the logarithmic divergence as $\theta \to 0$.

Expanding ϵ in powers of $\ln(z/z_0)$, we obtain

$$\epsilon(z) = \frac{2}{\ln(z/z_0)}\left(1 - \frac{\ln\ln(z/z_0)}{2\ln(z/z_0)} + \frac{\ln 2}{2\ln(z/z_0)} + \cdots\right), \tag{5.7}$$

and from (3.8), the corresponding series for w_0 is

$$w_0(z) = \left(\frac{B\ln(z/z_0)}{4\pi\nu}\right)^{1/2}\left(1 + \frac{\ln\ln(z/z_0)}{4\ln(z/z_0)} - \frac{\ln 2}{4\ln(z/z_0)} + \cdots\right). \tag{5.8}$$

The $\ln\xi$ terms in (5.3) and (5.4) match already, because we have already matched the vertical force $F(z)$ (to leading order) between the inner and outer solutions. Equating the remaining $O(\epsilon)$ terms in (5.3) and (5.4), we obtain

$$A - \frac{\gamma}{2} = \ln 2 - \delta - \left(A - \tfrac{1}{2}\ln 2\right)\left[\tfrac{1}{2}\epsilon \ln\left(\epsilon^{-1/2}\frac{z}{z_0}\right)\right]. \tag{5.9}$$

Noting that the factor in square brackets is equal to unity by our choice of ϵ, we deduce that

$$A = \tfrac{1}{4}(\gamma + 3\ln 2 - 2\delta). \tag{5.10}$$

Recall that γ is Euler's constant, while $\delta = 1/2$ for the free-slip boundary condition, and $\delta = 1$ for the rigid case. As would be expected on physical grounds, the free-slip case has a slightly larger vertical velocity, but a slower rate of increase of this velocity as the plume rises away from the boundary.

We have now determined $\epsilon(z)$, $w_0(z)$ and A by matching. Substituting these expressions back into the results of § 3, we obtain the inner solution explicitly, accurate to $O(\epsilon)$. The full outer solution is derived to the same accuracy in Appendix B. The leading-order radial velocity is shown in figure 4, and streamlines for the outer flow are shown in figure 5.

6. Discussion and concluding remarks

6.1. *Summary*

In this paper, we have studied the form of an axisymmetric plume rising from a point source above a plane boundary in very viscous fluid. We find a vertical length scale

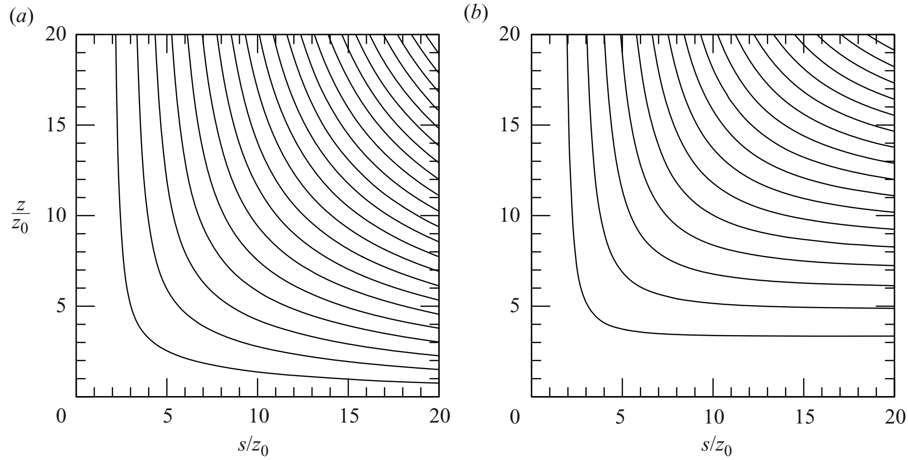

FIGURE 5. Stream-lines for the outer flow, including the zeroth and first-order terms ((B14)–(B18). (*a*) Corresponds to the free-slip boundary condition, whereas (*b*) is for the rigid case. Note that, since we are in an axisymmetric geometry, the velocities near the axis are higher than might initially be inferred from the stream-line separations (see figure 4).

$z_0 = (32\pi\kappa^2\nu/B)^{1/2}$, which is the scale on which advection becomes comparable with diffusion, and also on which the plume has an $O(1)$ aspect ratio. We have derived an asymptotic solution valid for $z \gg z_0$ by matching a slender plume region to the flow induced in the surrounding fluid. The plume width a is found to increase with height as $(z_0 z)^{1/2}\,[\ln(z/z_0)]^{-1/4}$, and the typical vertical velocity in plume w_0 increases slowly as $(B/\nu)^{1/2}\,[\ln(z/z_0)]^{1/2}$. The condition on the tangential velocity at the lower boundary is found to have no effect on the leading-order terms, and enters only at first order in a slender-body expansion in inverse powers of $\ln(z/z_0)$. We have calculated these first-order correction terms for both rigid and free-slip boundary conditions. Since slender-body expansions are only slowly converging, the second-order corrections may be a few per cent even at $z = 100z_0$.

The vertical velocity within the plume has two distinct components. First, there is a horizontally uniform component w_0. This is required to match the velocity in the outer fluid, which in turn is a global response to the buoyancy forces inside the plume. Secondly, there is a non-uniform component $\tilde{w}$, which is driven directly by the local buoyancy forces in the plume (via the Stokes equation). With the uniform viscosity considered here, the facts that the plume is slender and that w (and its derivative) must be matched to an outer flow with $O(1)$ aspect ratio means that $w_0 \gg \tilde{w}$ and the uniform component dominates. This was shown in § 2.3, and underpins the series expansion in ϵ that is used in this analysis.

6.2. *Effects of temperature-dependent viscosity*

If the viscosity decreases with temperature, then $\tilde{w}$ will have a larger curvature and is able to be larger near the centre of the plume without increasing the shear stress near the edge. It is now quite possible that $\tilde{w}$ will dominate w_0 in a central region near the axis (see figure 6). With a sufficiently large viscosity contrast, this central region can provide the main contributions to the vertical heat and mass fluxes. The uniform component w_0 (and hence the whole outer flow and associated matching problem) can then be neglected. This case of strong viscosity variation has been studied by

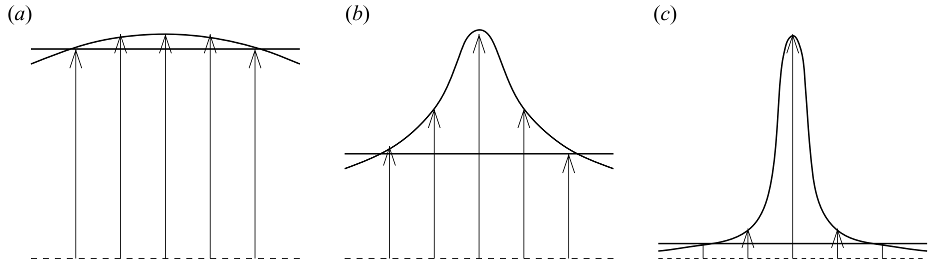

FIGURE 6. Expected vertical velocity profiles within a plume with (*a*) uniform viscosity, and (*b*, *c*) with increasing temperature-dependent viscosity contrasts. The velocity profiles are shown normalized by the centreline velocity. However, it may be more natural to consider the uniform component (which is set mainly by the outer viscosity) to have the same order of magnitude in some comparisons of the three cases.

Loper & Stacey (1983) and Olson *et al.* (1993), under the approximation that the narrow inner conduit sees little radial variation in temperature.

The method employed in the present work can easily be extended to cover the case of weak viscosity variation in which $\tilde{w} \ll w_0$ still holds. The leading-order result is unaltered, but many of the integrals for the first-order corrections would need to be calculated numerically. It would be more interesting to consider the intermediate case (depicted in figure 6*b*) where w_0 and $\tilde{w}$ are comparable, since this regime covers the transition from large viscosity contrast to uniform viscosity.

We note, however, that as z increases both the aspect ratio of the plume and the centreline temperature decrease. These effects both serve to decrease the magnitude of the non-uniform component $\tilde{w}$ relative to the uniform component w_0. Thus, for sufficiently large z, any plume should be well approximated by the uniform viscosity solution obtained here.

6.3. *Consideration of inertial effects*

Unlike the case of an isolated plume (see Worster 1986), we have obtained a solution without the necessity of including inertial effects in the far field. Nevertheless, if the Prandtl number is finite, inertia starts to play a role sufficiently far from the source.

The vertical velocity within the plume increases logarithmically with height. This is compensated for by the increasingly parallel nature of the flow, such that the effective Reynolds number $(ww_z)/(\nu\nabla_h^2\tilde{w})$ in the plume is $O(Pr^{-1})$ (see equations (2.7) and (2.8)) and hence small. However, outside the plume, the increasing length scale r of the flow dominates the slow logarithmic decrease of the velocity, so that inertial effects must be reintroduced in the external flow when

$$\frac{r}{z_0} \approx Pr\,(\ln Pr)^{1/2}\,. \tag{6.1}$$

It should be noted that the inertial corrections at very large distances do not have a leading-order effect on the flow within the radius given by (6.1), in much the same way that the Oseen correction for a translating sphere does not affect the Stokes solution near the sphere. The solution described in this paper is thus the appropriate asymptotic description out to $r = O(z_0 Pr(\ln Pr)^{1/2})$; at greater distances, inertial effects influence the velocity outside the plume and the appropriate description is that of Worster (1986).

Appendix A. Eigenmode corrections to a Gaussian buoyancy distribution

The temperature distribution in the plume is a result of advective and diffusive effects acting on the initial temperature profile emerging from the source. As we observed in §3, at leading order the advective effects correspond to those due to a uniform flow. We therefore expect the details of the initial profile to be lost as z increases, and the temperature distribution to relax towards the Gaussian form (3.15).

In §3, it was reasonably clear that the leading-order solution to (3.5) for $\epsilon \ll 1$ should be $f_0 = \xi^2/2$ corresponding to uniform flow. It was less clear that the leading-order solution to (3.6) for g should also be independent of z, as assumed in (3.10). If we relax this assumption, then we obtain the equation

$$(\xi g_0')' + 4\xi\left(g_0 - z g_{0z}\right) + 2\xi^2 g_0' = 0. \tag{A 1}$$

The general solution of (A 1) that is regular at $\xi = 0$ and decays as $\xi \to \infty$ may be written as the sum of separable solutions

$$g_0(\xi\,; z) = \sum_{n=0}^{\infty} \frac{\alpha_n}{z^n} G_n(\xi) \exp(-\xi^2), \tag{A 2}$$

where

$$G_n'' + \left(\frac{1}{\xi} - 2\xi\right) G_n' + 4n G_n = 0. \tag{A 3}$$

Equation (A 3) is the two-dimensional analogue of the Hermite equation, which arises in separable solution of the diffusion equation in one and three dimensions. With a suitable normalization, the functions G_n are related to the Laguerre polynomials L_n by $G_n(\xi) = L_n(\xi^2)$, and are thus polynomials of degree $2n$ which are orthogonal on $(0, \infty)$ with weight function $\xi \exp(-\xi^2)$. The first few are

$$G_0(\xi) = 1, \quad G_1(\xi) = 1 - \xi^2, \quad G_2(\xi) = 1 - 2\xi^2 + \tfrac{1}{2}\xi^4. \tag{A 4}$$

The analysis of §3 is based on retaining only the z-independent mode $n = 0$. The physical significance of the other modes is that they describe diffusive relaxation of g_0 with z from some initial profile towards the Gaussian profile (3.15). We note that there is a near-source region at the base of the plume of size $a \sim z \sim z_0$ in which the full Stokes and heat equations (2.1) and (2.3) must be solved. Treating the temperature profile emerging from this region as the initial profile for g_0, we find that $\alpha_n = O(z_0^n)$ and hence the neglected modes decay as $(z_0/z)^n$ for $n \geqslant 1$. Since the slender-body expansion of the flow is in inverse powers of $\ln(z/z_0)$, these algebraically decaying modes are asymptotically negligible.

The diffusive relaxation of the temperature distribution is more significant in the case of a distributed source studied in Part 2. There we find a critical height z^*, which is much larger than the length scale of the source. For $z \ll z^*$, the heat equation is dominated by advective terms, and diffusive effects only re-enter at $z = O(z^*)$. The eigenmode expansion (A 2) describes the diffusive relaxation of the plume for $z \gtrsim z^*$and provides an alternative to the solution by a Green's function (see the Appendix of Part 2).

Appendix B. Calculation of the full outer velocity field

Having determined $\epsilon(z)$, $w_0(z)$ and A in §5 (see equations (5.7), (5.8) and (5.10)), the interior buoyancy distribution is known explicitly up to first order as a function of s and z. Using a suitable expansion in inverse powers of $\ln(r/z_0)$, it is now possible to calculate the first few terms in an expansion of the outer velocity field $\boldsymbol{u}(r, \theta)$. We work from the multi-pole expansion (4.4) and the expression

$$F(z) = \left(\frac{4\pi\nu B}{\ln(z/z_0)}\right)^{1/2}\left(1 - \frac{\ln\ln(z/z_0)}{4\ln(z/z_0)} + \frac{\delta - \frac{1}{2}\gamma - \frac{1}{4}\ln 2}{\ln(z/z_0)} + \cdots\right), \tag{B 1}$$

for the Stokeslet line-density, which is derived from (4.7). The contributions from $M(z)$ and higher moments are algebraically small in r/z, and so can safely be neglected outside the plume.

We note that, unlike the planar case analysed by Roberts (1977) and the convection cell of Umemura & Busse (1989), the vertical force in the plume has a non-trivial dependence on z, and the calculation of the external flow is therefore more complicated.

Only one velocity component needs to be found directly from (4.4); the full flow-field can then be recovered using incompressibility. We choose the horizontal component $u = \boldsymbol{u} \cdot \hat{\boldsymbol{e}}_s$ because the individual terms in its integral decay most rapidly, and there is no need to rely on inter-term cancellations to obtain convergence.

After changing variables to the more natural spherical polar coordinates (r, θ, ϕ), we obtain

$$u(r, \theta) \sim \frac{1}{8\pi\nu}\int_0^\infty F(Xr)\,\Theta(\theta, X)\,\mathrm{d}X, \tag{B 2}$$

where $X = z'/r$, and for the free-slip boundary condition

$$\Theta(\theta, X) = \frac{\sin\theta(\cos\theta - X)}{(1 - 2X\cos\theta + X^2)^{3/2}} - \frac{\sin\theta(\cos\theta + X)}{(1 + 2X\cos\theta + X^2)^{3/2}}, \tag{B 3}$$

while for the rigid boundary condition

$$\Theta(\theta, X) = \frac{\sin\theta(\cos\theta - X)}{(1 - 2X\cos\theta + X^2)^{3/2}} - \frac{\sin\theta(\cos\theta - X)}{(1 + 2X\cos\theta + X^2)^{3/2}} - \frac{6\sin\theta\cos\theta(\cos\theta + X)X}{(1 + 2X\cos\theta + X^2)^{5/2}}. \tag{B 4}$$

In both cases, the form of $\Theta(\theta, X)$ is such that the dominant contribution to the integral occurs at $X = O(1)$ (i.e. $z' = O(r)$) rather than $X \ll 1$ or $X \gg 1$. Physically, this is because of the near cancellation of the Stokeslet and its image for points much closer or farther away from the origin than the point (r, θ) under consideration. We therefore expand $F(Xr)$ for $z_0/r \ll X \ll r/z_0$, using (B 1) and

$$[\ln(Xr/z_0)]^\alpha = [\ln(r/z_0)]^\alpha\left(1 + \frac{\alpha\ln(X)}{\ln(r/z_0)} + \cdots\right). \tag{B 5}$$

It is this step that was not possible in § 4 before the form of ϵ, w_0, and hence F were known.

Equation (B 2) is then rewritten as a series of integrals, whose dependence on r can be separated from the integrands. We obtain

$$u(r, \theta) \sim \left(\frac{B}{16\pi\nu\ln(r/z_0)}\right)^{1/2}\left\{U_0(\theta)\left(1 - \frac{\ln\ln(r/z)}{4\ln(r/z_0)}\right) + \frac{U_1(\theta)}{\ln(r/z_0)} + \cdots\right\}, \tag{B 6}$$

where

$$U_0(\theta) = \int_0^\infty \Theta(\theta, X)\,\mathrm{d}X, \tag{B 7}$$

$$U_1(\theta) = -\frac{1}{2}\int_0^\infty \Theta(\theta, X)\,\ln X\,\mathrm{d}X + \left(\delta - \tfrac{1}{2}\gamma - \tfrac{1}{4}\ln 2\right)U_0(\theta). \tag{B 8}$$

For the free-slip case we obtain

$$U_0(\theta) = -2\sin\theta, \tag{B 9}$$

$$U_1(\theta) = -\sin\theta\,\ln\left(\tfrac{1}{2}\sin\theta\right) + \left(\delta - \tfrac{1}{2}\gamma - \tfrac{1}{4}\ln 2\right)U_0(\theta), \tag{B 10}$$

whereas for the rigid case

$$U_0(\theta) = -2\sin\theta + \frac{2(1-\cos\theta)^2}{\sin\theta}, \tag{B 11}$$

$$U_1(\theta) = -\sin\theta\,\ln\left(\tfrac{1}{2}\sin\theta\right) + \frac{(1+\cos\theta)^2}{\sin\theta}\ln\left(\cos\tfrac{1}{2}\theta\right) + \frac{(1-\cos\theta)\cos\theta}{\sin\theta} + \left(\delta - \tfrac{1}{2}\gamma - \tfrac{1}{4}\ln 2\right)U_0(\theta). \tag{B 12}$$

The Stokes streamfunction $\Psi(r,\theta)$ is obtained from u by integration of

$$u = \frac{1}{r^2}\frac{\partial\Psi}{\partial\theta} - \frac{\cos\theta}{r\sin\theta}\frac{\partial\Psi}{\partial r}. \tag{B 13}$$

Since there is no vertical flow across the horizontal boundary $\theta = \pi/2$, we may impose $\Psi(r, \pi/2) = 0$ without loss of generality. This condition determines the constant of integration, and we obtain

$$\Psi(r,\theta) = \left(\frac{B}{4\pi\nu\ln(r/z_0)}\right)^{1/2} r^2\left\{\Psi_0(\theta)\left(1 - \frac{\ln\ln(r/z_0)}{4\ln(r/z_0)}\right) + \frac{\Psi_1(\theta)}{\ln(r/z_0)} + \cdots\right\}. \tag{B 14}$$

With the free-slip boundary condition, we have

$$\Psi_0(\theta) = \sin^2\theta\,\ln\cot\tfrac{1}{2}\theta, \tag{B 15}$$

$$\Psi_1(\theta) = -\sin^2\theta\left(\ln\left(\tan\tfrac{1}{2}\theta\right)\ln\left(\sec\tfrac{1}{2}\theta\right) + \tfrac{1}{2}\mathrm{Li}_2\left(-\tan^2\tfrac{1}{2}\theta\right) + \frac{\pi^2}{24}\right) + \left(\delta - \tfrac{1}{2}\gamma - \tfrac{1}{4}\ln 2\right)\Psi_0(\theta), \tag{B 16}$$

whereas for the rigid case

$$\Psi_0(\theta) = \sin^2\theta\,\ln\cot\tfrac{1}{2}\theta - (1-\cos\theta)\cos\theta, \tag{B 17}$$

$$\Psi_1(\theta) = -\sin^2\theta\left(\ln\left(\tan\tfrac{1}{2}\theta\right)\ln\left(\sec\tfrac{1}{2}\theta\right) + \tfrac{1}{2}\mathrm{Li}_2\left(-\tan^2\tfrac{1}{2}\theta\right) + \frac{\pi^2}{24}\right) - \cos\theta(1+\cos\theta)\ln\left(\cos\tfrac{1}{2}\theta\right) + \left(\delta - \tfrac{1}{2}\gamma - \tfrac{1}{4}\ln 2\right)\Psi_0(\theta), \tag{B 18}$$

where $\mathrm{Li}_2(z) = \int_z^0 t^{-1}\ln(1-t)\,\mathrm{d}t$ is a dilogarithm. As before, $\delta = 1/2$ and 1, respectively, for the free-slip and rigid boundary conditions. The stream-lines of this outer flow are plotted for each boundary condition in figure 5. The leading-order radial velocity is shown in figure 4. It may be verified that the vertical velocity computed from (B 14) is consistent with the asymptotic limit for $\theta \ll 1$ which was derived in § 4.3.

By repeating the calculations above with $F(z) = F_0$, it is easy to show that the stream function for a uniform Stokeslet line-density along the axis is given by

$$\Psi(r,\theta) = \frac{F_0}{4\pi\nu}r^2\,\Psi_0(\theta), \tag{B 19}$$

where $\Psi_0(\theta)$ is as defined in (B 15) or (B 17) depending on the lower boundary condition. Therefore, at the point (r_0, θ_0), the leading-order outer velocity for a point-source plume is equal to the velocity that would occur there when driven by a uniform Stokeslet distribution along the axis with line-density $F_0 = F(r_0)$. This reinforces the earlier observation that the leading-order contribution to the velocity at radius r comes from the forcing on the axis at height $z = O(r)$. This is expected to hold for any logarithmically slowly varying Stokeslet distribution along the axis, i.e. the leading-order streamfunction for such a distribution $\mathscr{F}(z)$ is given by

$$\Psi(r, \theta) \sim \frac{\mathscr{F}(r)}{4\pi\nu} r^2 \Psi_0(\theta). \tag{B 20}$$

We shall make use of this result in Part 2.

REFERENCES

Blake, J. R. 1971 A note on the image system for a Stokeslet in a no slip boundary. *Proc. Camb. Phil. Soc.* **70**, 303.

Cox, R. G. 1970 The motion of long slender bodies in a viscous fluid. Part 1. General theory. *J. Fluid Mech.* **44**, 791–810.

Kaminski, E. & Jaupart, C. 2003 Laminar starting plumes in high-Prandtl-number fluids. *J. Fluid Mech.* **478**, 287–298.

Kerr, R. C. & Mériaux, C. 2004 Structure and dynamics of sheared mantle plumes. *Geochem. Geophys. Geosyst.* **5** (12).

Krause, D. & Loch, H. (ed.) 2002 *Mathematical Simulation in Glass Technology*. Springer.

Lamb, H. 1911 On the uniform motion of a sphere through a viscous fluid. *Phil. Mag. (Ser. 6)* **21** (121), 112–121.

Leal, L. G. 1992 *Laminar Flow and Convective Transport Processes*. Butterworth–Heinemann.

Loper, D. E. & Stacey, F. D. 1983 The dynamical and thermal structure of deep mantle plumes. *Phys. Earth Planet. Int.* **33**, 304–317.

Lorentz, H. A. 1907 Ein allgemeiner Satz, die Bewegung einer reibenden Flüssigkeit betreffend, nebst einigen Anwendungen desselben. In *Abhandlungen über Theoretische Physik*, pp. 23–42. B. G. Teubner, Leipzig, Berlin.

Morgan, W. J. 1971 Convection plumes in the lower mantle. *Nature* **230**, 42–43.

Olson, P., Schubert, G. & Anderson, C. 1993 Structure of axisymmetric mantle plumes. *J. Geophys. Res.* **98** (B4), 6829–6844.

Pozrikidis, C. 1992 *Boundary Integral and Singularity Methods for Linearized Viscous Flow*. Cambridge University Press.

Roberts, G. O. 1977 Fast viscous convection. *Geophys. Astrophys. Fluid Dyn.* **8**, 197–233.

Umemura, A. & Busse, F. H. 1989 Axisymmetric convection at large Rayleigh and infinite Prandtl number. *J. Fluid Mech.* **208**, 459–478.

Whittaker, R. J. & Lister, J. R. 2006 Steady axisymmetric creeping plumes above a planar boundary. Part 2. A distributed source. *J. Fluid Mech.* **567**, 379–397.

Worster, M. G. 1986 The axisymmetric laminar plume: asymptotic solution for large Prandtl number. *Stud. App. Maths* **75**, 139–152.